

# MicroRNA-196a/b Mitigate Renal Fibrosis by Targeting TGF- $\beta$ Receptor 2

Jiao Meng,\* Limin Li,<sup>†</sup> Yue Zhao,\* Zhen Zhou,<sup>†</sup> Mingchao Zhang,\* Donghai Li,<sup>†</sup> Chen-Yu Zhang,<sup>†</sup> Ke Zen,<sup>†</sup> and Zhihong Liu\*

\*National Clinical Research Center of Kidney Diseases, Jinling Hospital, School of Medicine, Nanjing University, Nanjing, China; and <sup>†</sup>State Key Laboratory of Pharmaceutical Biotechnology, Jiangsu Engineering Research Center for MicroRNA Biology and Biotechnology, School of Life Science, Nanjing University, Nanjing, China

## ABSTRACT

Organ-specific microRNAs have essential roles in maintaining normal organ function. However, the microRNA profile of the kidney and the role of microRNAs in modulating renal function remain undefined. We performed an unbiased assessment of the genome-wide microRNA expression profile in 14 mouse organs using Solexa deep sequencing and found that microRNA-196a (miR-196a) and miR-196b are selectively expressed in kidney, with 74.37% of mouse total miR-196a and 73.19% of mouse total miR-196b distributed in the kidneys. We confirmed the predominant expression of miR-196a/b in mouse and human kidney, particularly in the glomeruli and tubular epithelium, by quantitative RT-PCR and *in situ* hybridization assays. During unilateral ureteral obstruction (UUO)-induced mouse renal fibrosis, renal miR-196a/b levels rapidly decreased. Elevation of renal miR-196a/b expression by hydrodynamic-based delivery of a miR-196a/b-expressing plasmid before or shortly after UUO significantly downregulated profibrotic proteins, including collagen 1 and  $\alpha$ -smooth muscle actin, and mitigated UUO-induced renal fibrosis. In contrast, depletion of renal miR-196a/b by miR-196a/b antagomirs substantially aggravated UUO-induced renal fibrosis. Mechanistic studies further identified transforming growth factor beta receptor II (TGF $\beta$ R2) as a common target of miR-196a and miR-196b. Decreasing miR-196a/b expression in human HK2 cells strongly activated TGF- $\beta$ -Smad signaling and cell fibrosis; whereas increasing miR-196a/b levels in mouse primary cultured tubular epithelial cells inhibited TGF- $\beta$ -Smad signaling. In the UUO model, miR-196a/b silenced TGF- $\beta$ -Smad signaling, decreased the expression of collagen 1 and  $\alpha$ -smooth muscle actin, and attenuated renal fibrosis. Our findings suggest that elevating renal miR-196a/b levels may be a novel therapeutic strategy for treating renal fibrosis.

*J Am Soc Nephrol* 27: 3006–3021, 2016. doi: 10.1681/ASN.2015040422

MicroRNAs (miRNAs) are noncoding RNAs of approximately 22 nucleotides in length that target specific mRNA sequences and suppress gene expression at the post-transcriptional level.<sup>1,2</sup> It has been extensively shown that miRNAs play critical roles in regulating a variety of cellular developmental and physiologic processes.<sup>3,4</sup> In humans and animals, particular organs are enriched for specific miRNAs, and these organ-enriched miRNAs are essential for maintaining the normal physiologic function of the organ. For example, >70% of microRNA-122 (miR-122) is found

Received April 19, 2015. Accepted January 10, 2016.

J.M., L.L., Y.Z., and Z.Z. contributed equally to this work.

Published online ahead of print. Publication date available at [www.jasn.org](http://www.jasn.org).

**Correspondence:** Prof. Zhihong Liu, National Clinical Research Center of Kidney Diseases, Jinling Hospital, Nanjing University School of Medicine, Nanjing, Jiangsu 210009, China, or Prof. Ke Zen, Jiangsu Engineering Research Center for MicroRNA Biology and Biotechnology, State Key Laboratory of Pharmaceutical Biotechnology, School of Life Sciences, Nanjing University, Nanjing, Jiangsu 210093, China. Email: [liuzhihong@nju.edu.cn](mailto:liuzhihong@nju.edu.cn) or [kzen@nju.edu.cn](mailto:kzen@nju.edu.cn)

Copyright © 2016 by the American Society of Nephrology

in the liver,<sup>5</sup> where miR-122 plays a critical health-promoting role by suppressing tumorigenesis and uncontrolled proliferation and inflammation.<sup>6,7</sup> In an analogous fashion, the brain selectively expresses miR-124a and miR-9,<sup>8</sup> whereas muscle tissue selectively expresses miR-1 and miR-133.<sup>5</sup> Recent studies report that a panel of miRNAs, including miR-10a/b, miR-200a, miR-196a/b, miR-335, miR-192, miR-194, miR-204, miR-215, and miR-216, is enriched in kidney tissues<sup>8,9</sup>; however, the function of these miRNAs requires clarification.

Renal fibrosis is the common end stage of various CKDs. Renal tubulointerstitial fibrosis is characterized by leukocyte infiltration, tubular cell apoptosis and necrosis, tubulointerstitial fibroblast proliferation, and extracellular matrix (ECM) deposition.<sup>10–15</sup> The severity of renal fibrosis tightly correlates with the degree of renal dysfunction and the risk for renal failure progression.<sup>16</sup> TGF- $\beta$  plays a very important role in the pathogenesis of renal fibrosis.<sup>17–20</sup> The profibrotic effect of upregulated TGF- $\beta$  is mainly mediated through the activation of TGF- $\beta$ –Smad signaling pathways.<sup>21</sup> Briefly, TGF- $\beta$  binds to TGF- $\beta$  receptor 2 (TGF $\beta$ R2) in the kidney. After ligand binding, the TGF $\beta$ R2 triggers the phosphorylation and activation of downstream signaling mediators Smad2 and Smad3. Phosphorylated Smad2/3 bind to Smad4 proteins forming hetero-oligomeric complexes, which subsequently translocate into the cell's nucleus, where they induce transcription of fibrotic genes.<sup>18,22</sup> Recent studies suggest that, after gene transcription, miRNAs regulate the translation of various mRNAs into proteins involved in kidney fibrosis. Certain miRNAs downstream of TGF- $\beta$  signaling (*viz.*, miR-192 and miR-377) are associated with initiation and progression of kidney fibrosis in patients with diabetic nephropathy (DN) and in animal models of diabetic nephropathy.<sup>23–25</sup> In contrast, miRNAs belonging to the miR-200 and miR-29 families display antifibrotic effects in the progression of renal fibrosis disease.<sup>23,24,26–28</sup>

In this study, we performed an unbiased assessment of whole-genome miRNA expression in 14 major mouse organs using Solexa deep sequencing, and compared the distribution of individual miRNAs in various organs to distinguish the kidney-enriched miRNAs. The results showed that miR-196a and miR-196b are predominantly expressed in the kidney. We further confirmed the presence of miR-196a/b in the kidney by *in situ* hybridization and TaqMan probe-based real time RT-PCR using both human and mouse kidneys. We next explored the role of miR-196a/b in renal fibrosis using the unilateral ureteral obstruction mouse model. Both miR-196a and miR-196b rapidly declined after ureteral obstruction, suggesting that miR196a/b may protect against fibrosis of the kidney. We next identified TGF $\beta$ R2 mRNA as the common target of miR-196a and miR-196b. Thus, our *in vivo* and *in vitro* results were consistent with the conclusion that kidney-predominant miR-196a/b can protect against the development of mouse renal fibrosis *via* limiting the binding of TGF- $\beta$  to the TGF $\beta$ R2 receptor and the downstream consequences of TGF $\beta$ R2 signaling.

## RESULTS

### miR-196a and miR-196b Are Predominantly Expressed in the Kidney

In order to identify miRNAs that are selectively expressed in the kidney, we analyzed the expression profiles of miRNAs at whole-genome level by Solexa sequencing in 14 mouse organs, including heart, liver, kidney, stomach, spleen, cerebrum, cerebellum, small intestine, lung, pancreas, ovary, colon, esophagus, and uterus (GEO accession number: GSE67885). Solexa data showed that a panel of miRNAs, including let-7a, miR-143, miR-196b, miR-21, miR-378, miR-29a, miR-27b, miR-148a, and miR-30a, was highly expressed in the mouse kidney (Figure 1A, Supplemental Tables 1 and 2). Honing in to distinguish miRNAs unique to the kidney, we compared the level of these miRNAs across various organs. We found that 74.37% of the miR-196a in the mouse and 73.19% of the miR-196b in the mouse were located in the kidney (Figure 1B, Supplemental Table 3). Previous reports by ourselves<sup>29</sup> and others<sup>30</sup> showed that the kidney expressed high levels of miR-30–family miRNAs, which played a critical role in maintaining podocyte function. Indeed, our Solexa sequencing data confirmed that the mouse kidney expresses a high level of miR-30 family–member miRNAs. For instance, kidney miR-30a comprised >30% of total mouse miR-30a. We confirmed the specificity of miR-122 for the liver (miR-122 served as a control for liver-specific miRNA) by Solexa sequencing. To validate the findings of Solexa sequencing, we performed TaqMan probe-based real-time PCR assays on miR-196a and miR-196b in various mouse organs. As shown in Figure 1C, consistent with the results from Solexa analysis, miR-196a and miR-196b were highly expressed in the kidney compared with other mouse organs.

To further identify the distribution of miR-196a and miR-196b in the kidney, *in situ* hybridization was performed using kidney tissue sections from healthy mice and healthy humans. Results clearly showed that miR-196a and miR-196b were strongly expressed in both glomerular and tubular interstitial cells (Figure 2A, arrows). We also performed a TaqMan probe-based qRT-PCR assay using microdissected mouse or human glomerular and tubular interstitial fractions, and the results confirmed that both glomerular and tubular interstitial fractions contain abundant levels of miR-196a and miR-196b (Figure 2B, Supplemental Figure 1).

### Protective Function of miR-196a/b in Unilateral Ureteral Obstruction–Induced Mouse Renal Fibrosis

The unilateral ureteral obstruction (UUO) model is a well established model of experimental renal fibrosis. To explore the role of miR-196a/b in renal fibrosis, we used the UUO mouse model. We obstructed the ureter exiting the right kidney. The observed dilation of the pelvis and proximal ureter and the collapse of the distal ureter confirmed the success of this obstruction. As shown in Figure 3, A and B, Masson trichrome staining and anti-CD11b staining revealed that, compared with normal mice, the UUO-treated mice all displayed typical features of renal hydronephrosis, fibrosis, and the infiltration

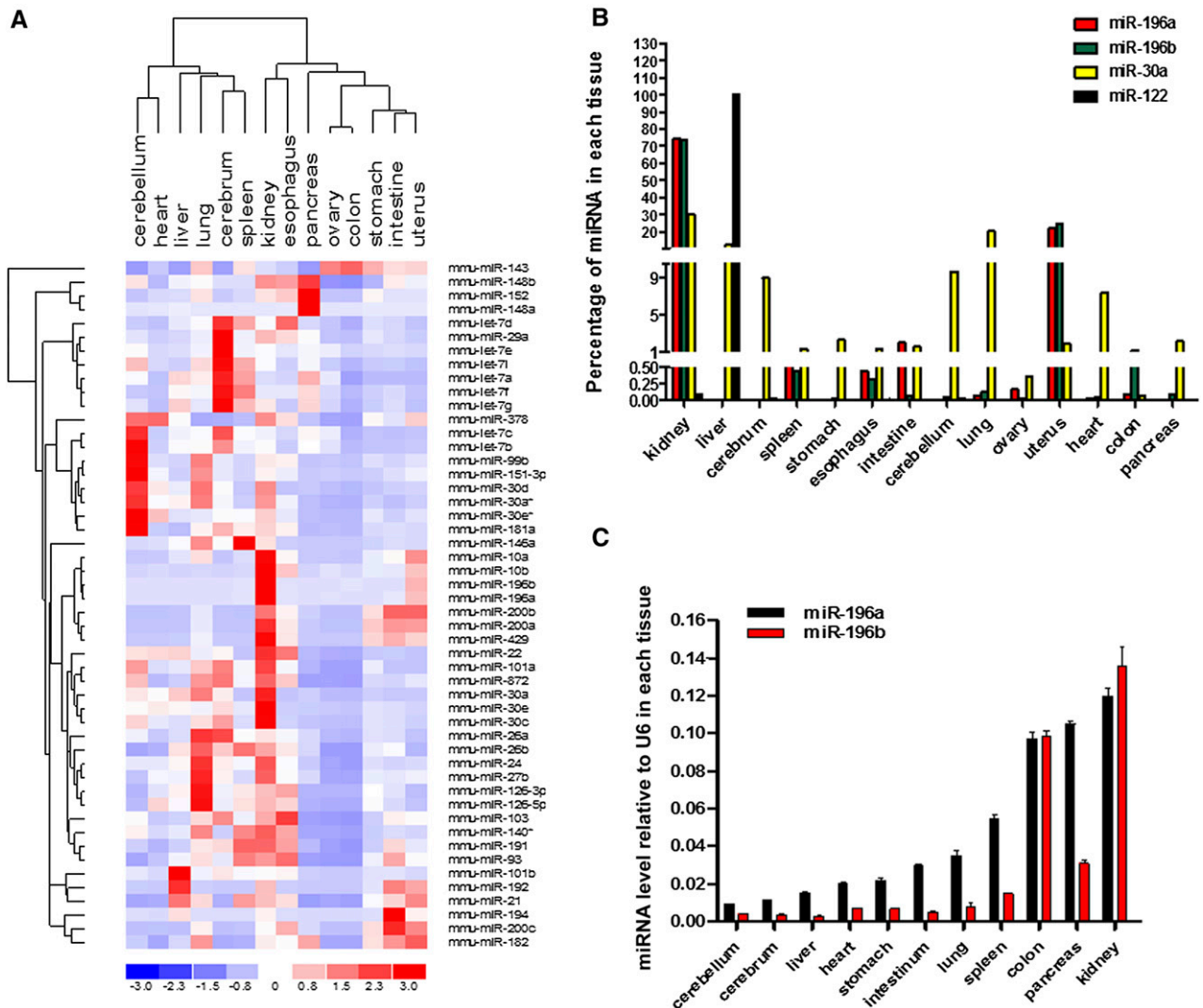


**Figure 1.** miR-196a and miR-196b are highly selectively expressed in mouse kidney. In this experiment, we analyzed the whole-genome miRNA expression profile in various mouse organs by Solexa deep sequencing. (A) Heat map of the clustering of miRNA expression profile in various mouse organs. We selected the miRNAs with sequencing reads ranked top 50 in kidney. (B) Distribution of mouse miR-196a, miR-196b, miR-30a, and miR-122 in various mouse organs. We calculated the percentage of miRNA as copy number of individual miRNA (e.g., miR-196a) in one tissue (e.g., kidney)/copy number of the same miRNA in all 14 tissues. (C) Validation of the expression of miR-196a and miR-196b in mouse organs by TaqMan probe-based qRT-PCR. We normalized the levels of miR-196a and miR-196b to U6 in different tissues (we calculated the expression level as  $2^{-\Delta Ct}$ ,  $\Delta Ct = Ct_{miRNA} - Ct_{U6}$ ). Results are presented as mean  $\pm$  SEM from three independent experiments.

of inflammatory cells (Figure 3B). We then isolated total RNAs from mouse kidneys harvested on days 0, 3, and 7 after the UUO procedure. We used real-time PCR analysis to measure the expression of renal miR-196a and miR-196b. The results demonstrated that miR-196a and miR-196b levels were significantly downregulated after the procedure (Figure 3C). As shown in Figure 3D, the *in situ* hybridization study further confirmed the decrease of miR-196a and miR-196b levels in the glomeruli and the renal tubular epithelium in UUO mice.

On the basis of our results, we postulated that miR-196a and miR-196b might negatively modulate the process of renal fibrosis. To test this hypothesis, we prevented the UUO-

induced reduction of miR-196a and miR-196b in mouse kidney by delivering miR-196a/b-expressing plasmids into the kidneys *via* a tail vein injection<sup>31</sup> before the UUO procedure (Figure 4A). Delivery of miR-196a/b-expressing plasmids effectively increased the levels of miR-196a and miR-196b in the mouse kidney (Supplemental Figure 2). As shown in Figure 4B, injection of miR-196a/b-expressing vectors completely rescued the reduction of miR-196a and miR-196b in mouse kidneys on day 7 after the UUO procedure. In control animals, injection with empty control vector did not rescue the reduction of mouse kidney miR-196a/b induced by the UUO procedure. We next investigated the effect of miR-196a and miR-196b rescue on UUO-induced mouse renal fibrosis. As

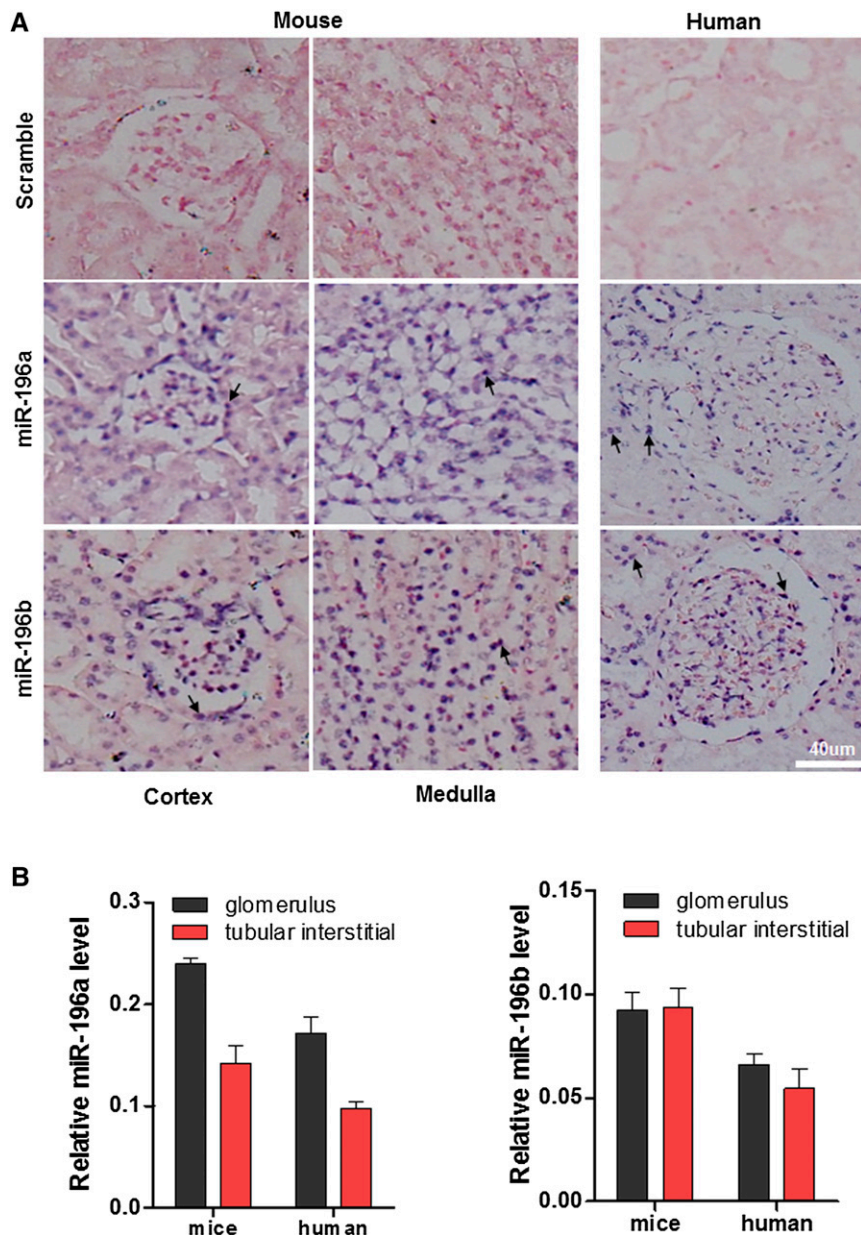


**Figure 2.** Enrichment of miR-196a and miR-196b in mouse and human kidney. (A) Localization of miR-196a and miR-196b in mouse and human kidney analyzed by *in situ* hybridization. We used double digoxigenin-labeled locked miR-196a or miR-196b probes to detect the level of miR-196a or miR-196b. Note that glomerulus and tubular epithelium in both mouse and human abundantly express miR-196a and miR-196b (arrows). Magnification,  $\times 400$ . (B) Validation of preferential expression of miR-196a and miR-196b in isolated mouse or human renal glomerulus and tubular interstitial cells by qRT-PCR. We normalized the levels of miR-196a and miR-196b to U6 (we calculated the expression level as  $2^{-\Delta Ct}$ ,  $\Delta Ct = Ct_{miRNA} - Ct_{U6}$ ). Results are presented as mean  $\pm$  SEM from three independent experiments.

shown by Masson trichrome staining and anti-CD11b staining of mouse renal tissue sections in Figure 4, C and D, delivery of miR-196a/b-expressing plasmids significantly mitigated the severity of tubular interstitial fibrosis and the infiltration of inflammatory cells (Figure 4D) induced by UUO. These

results suggest that delivery of miR-196a and miR-196b can significantly prevent renal fibrosis.

To further validate the protective effect of miR-196a and miR-196b on UUO-induced renal fibrosis, we also injected mice with miR-196a/b antagonomirs and miR-196a/b-expressing plasmids after the UUO procedure (Figure 5A). As shown in Figure 5B, injection of miR-196a/b-expressing plasmids on day 7 after the UUO procedure completely rescued the reduction of miR-196a and miR-196b in mouse kidneys induced by UUO, whereas injection of miR-196a/b antagonomirs enhanced the reduction of miR-196a and miR-196b. The Masson trichrome staining and anti-CD11b staining assay (Figure 5, C and D) further showed that miR-196a/b-expressing plasmids alleviated, whereas miR-196a/b antagonomirs aggravated, the severity of tubular interstitial fibrosis and the infiltration of inflammatory cells (Figure 5D) induced by UUO. These results indicate that delivery of miR-196a and miR-196b after a UUO procedure can mitigate renal fibrosis. Therefore, elevating renal miR-196a/b levels may offer a novel therapeutic strategy for treating renal fibrosis.

#### Human and Mouse TGF $\beta$ R2 mRNA Is a Common Target of miR-196a and miR-196b

We predicted the potential targets of miR-196a and miR-196b using a combination of several software programs, including TargetScan, miRDB, and miRanda.<sup>32–35</sup> Our three software programs consistently predicted the mRNA of TGF $\beta$ R2, an essential receptor at the early stage of the profibrotic TGF- $\beta$  signaling pathway, and thus we elected to further investigate how miR-196a/b influenced the expression of TGF $\beta$ R2. Although the base sequences in the 3'-UTR of TGF $\beta$ R2 mRNA are not highly conserved between human and mice, both human and mouse 3'-UTR mRNA for TGF $\beta$ R2 offer binding sites for miR-196a and miR-196b (Figure 6A). The seed region (the core sequences that encompass the first two to eight bases of the mature miRNA) of miR-196a and miR-196b all base-paired with the 3'-UTR of TGF $\beta$ R2 mRNA with a free energy of  $-22.8$  and  $-19.1$  kcal/mol for human, and  $-28.0$  and  $-25.1$  kcal/mol for mouse. To validate the binding of miR-196a/b to the human and the mouse TGF $\beta$ R2 3'-UTR, we amplified the full-length 3'-UTRs of human and mouse TGF $\beta$ R2



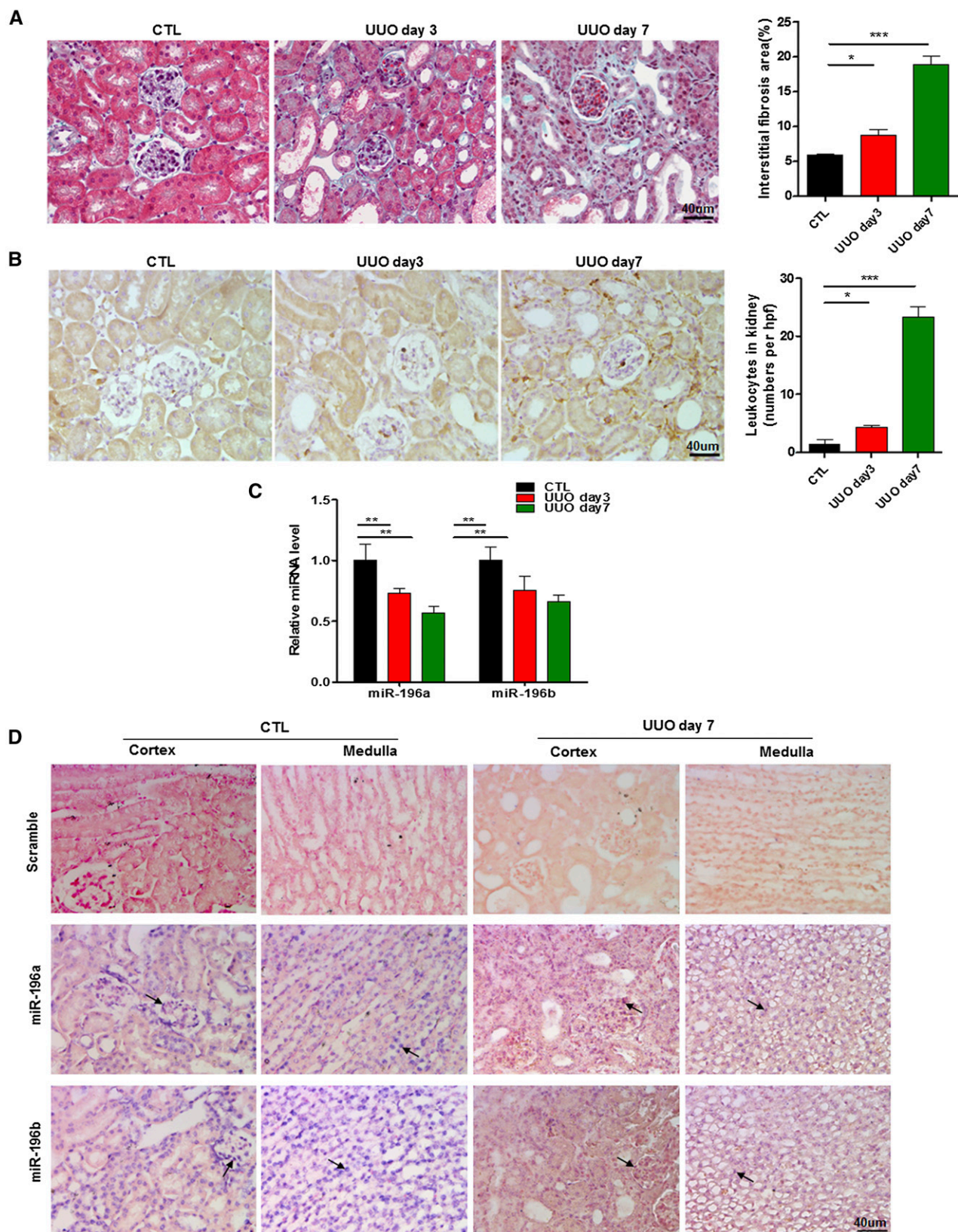


**Figure 3.** Decrease of miR-196a and miR-196b levels in mouse kidney during unilateral ureteral obstruction (UUO)-induced renal fibrosis. (A) Representative images of Masson trichrome staining of kidney without (CTL) or with UUO procedure at different time points. Magnification,  $\times 400$ . Right histogram represents quantitative analysis of tubular interstitial fibrosis from Masson trichrome staining

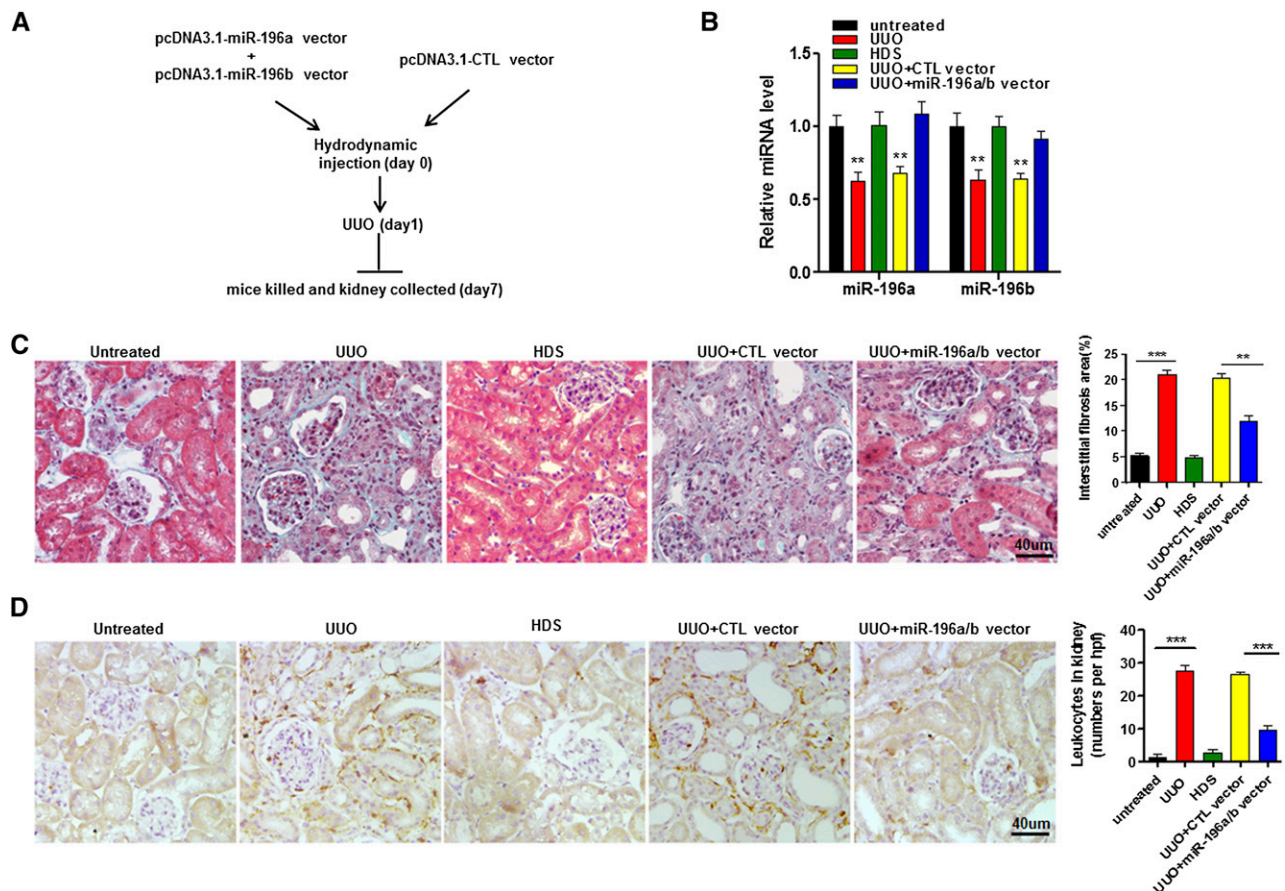


**Figure 4.** Overexpression of miR-196a and miR-196b before the UUO procedure prevented UUO-induced mouse renal fibrosis. We delivered the miR-196a/b–expressing vectors or control vector into mice via a previously described hydrodynamic-based gene-transfer technique.<sup>56</sup> (A) Schematic diagram of the experimental procedure. Mice were divided into five groups: mice without treatment (untreated), mice with UUO (UUO), mice without UUO and with transfer of hydrodynamic solution (HDS), mice with UUO and transfer with control vector (UUO+CTL vector), and mice with UUO and transfer with miR-196a– and miR-196b–expressing vector (UUO+miR-196a/b vector). (B) Levels of miR-196a and miR-196b in kidneys of UUO mice (day 7) transfected with miR-196a/b–expressing vector or control vector. Data are compared with untreated mice. (C) Representative images of Masson trichrome staining of kidney of UUO (day 7) mice transfected with miR-196a/b–expressing vector or control vector. Magnification,  $\times 400$ . Right histogram represents quantitative analysis of tubular interstitial fibrosis from Masson trichrome staining results. (D) Representative images of CD11b immune staining of kidney without (CTL) or with UUO procedure at different time points. Magnification,  $\times 400$ . Right histogram represents quantitative analysis of infiltrated myeloid cells from anti-CD11b staining results (six high-power fields counted per group). Results are presented as mean  $\pm$  SEM from three independent experiments. Each group consisted of five or six mice. \*\*\*P<0.001; \*\*P<0.01.

mRNA and then fused them downstream of the firefly luciferase gene in a reporter plasmid. We transfected the constructed human and mouse 3′-UTR reporter plasmids respectively into human renal proximal tubular epithelial HK2 cells and 293T cells, along with transfection of control plasmid ( $\beta$ -gal) and miR-196a/b mimic or inhibitor. As shown in Supplemental Figure 3,

transfection of miR-196a/b–expressing plasmids strongly increased miR-196a and miR-196b expression, whereas introduction of miR-196a/b antagonists depleted miR-196a and miR-196b. We transfected reporter constructs containing human 3′-UTR TGF $\beta$ R2 mRNA or mouse 3′-UTR TGF $\beta$ R2 mRNA into HK2 cells (Figure 6B) and 293T cells (Figure 6C), respectively.

results. (B) Representative images of anti-CD11b staining of kidney without or with UUO procedure at different time points. Magnification,  $\times 400$ . Right histogram represents quantitative analysis of infiltrated myeloid cells from anti-CD11b staining results (six high-power fields counted per group). (C) Relative expression levels of miR-196a and miR-196b in mouse kidney with or without UUO treatment at different times. Data are compared with untreated mice. (D) *In situ* hybridization of miR-196a and miR-196b in renal biopsy samples of mice before (CTL) or after UUO treatment. Note that the abundant expression of miR-196a and miR-196b (arrows) in CTL mouse glomerulus and renal tubular epithelium is significantly reduced after the UUO procedure. Magnification,  $\times 400$ . Results are presented as mean  $\pm$  SEM from three independent experiments. Each group consisted of five or six mice. \*P<0.05; \*\*P<0.01; \*\*\*P<0.001.



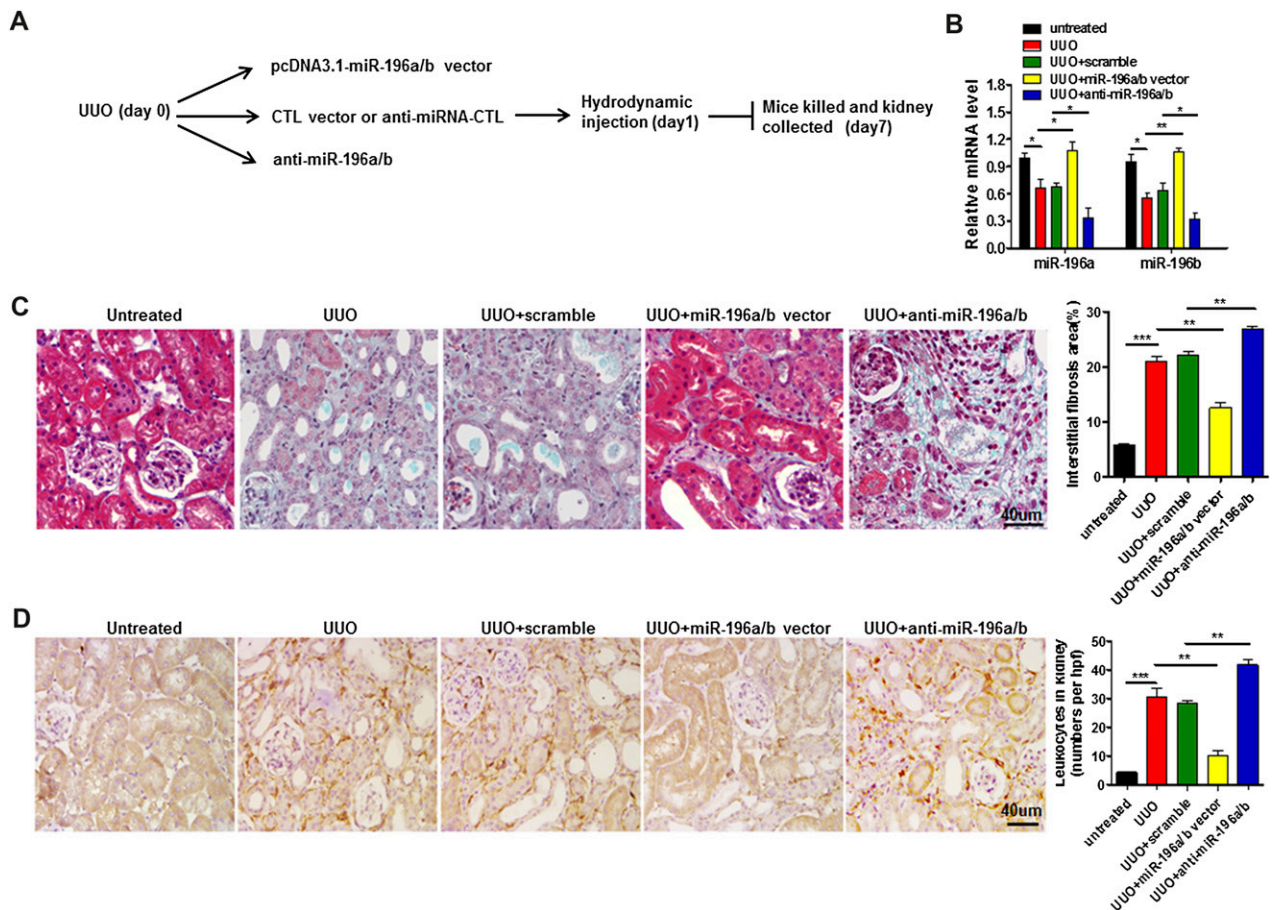


**Figure 5.** Role of overexpression or downregulation of miR-196a/b after the UUO procedure in alleviating or aggravating UUO-induced mouse renal fibrosis. We injected the miR-196a/b-expressing plasmids, miR-196a/b antagonists, or control plasmids into mice via a hydrodynamic-based gene-transfer technique. (A) Schematic diagram of the experimental procedure. Mice were divided into five groups: mice without treatment (untreated), mice with UUO procedure (UUO), mice with UUO procedure and scramble control (UUO+scramble), mice with UUO procedure and miR-196a/b-expressing plasmids (UUO+miR-196a/b vector), and mice with UUO procedure and miR-196a/b antagonists (UUO+anti-miR-196a/b). (B) Levels of miR-196a and miR-196b in mouse kidneys on day 7 post-UUO (all results are normalized against untreated mice). (C) Representative images of Masson trichrome staining of mouse kidneys (day 7 post-UUO). Magnification,  $\times 400$ . Right histogram represents quantitative analysis of tubular interstitial fibrosis from Masson trichrome staining. (D) Representative images of anti-CD11b staining of kidney without (CTL) or with UUO procedure at different time points. Magnification,  $\times 400$ . Right histogram represents quantitative analysis of infiltrated myeloid cells by anti-CD11b staining (six high-power fields counted per group). Results are presented as mean  $\pm$  SEM from three independent experiments. Each group consisted of five or six mice. \* $P < 0.05$ ; \*\* $P < 0.01$ ; \*\*\* $P < 0.001$ .

Luciferase reporter assays demonstrated that overexpression of miR-196a/b in HK2 and 293T cells suppressed approximately 30% of luciferase activity of the reporters containing the miR-196a and miR-196b recognition sequence, whereas cells transfected with miR-196a/b antagonists exhibited an approximately twofold increase in reporter activity compared with the cells transfected with control inhibitor (Figure 6, B and C). For further validation, we introduced point mutations into the miR-196a/b complementary sites within the human and mouse TGF $\beta$ 2 mRNA 3'-UTR, to eliminate the predicted binding sites for miR-196a and miR-196b. Reporter constructs containing the mutated human 3'-UTR TGF $\beta$ 2 mRNA or mutated mouse 3'-UTR TGF $\beta$ 2 mRNA were transfected into HK2 (Figure 6B)

and 293T cells (Figure 6C), respectively. The mutated luciferase reporter was unaffected by either the overexpression or the knock-down of miR-196a/b.

We then evaluated whether knockdown of both miR-196a and miR-196b would effect the expression of TGF $\beta$ 2. In this experiment, we transfected HK2 cells with equivalent amounts of either miR-196a antagonists or miR-196b antagonists or control oligonucleotides. Western blot analysis showed that the introduction of both the miR-196 antagonists significantly increased the levels of the TGF $\beta$ 2 protein at 24 hours post-transfection, relative to control oligonucleotides (Figure 6D). Because TGF $\beta$ 2 induces renal fibrosis by first initiating the phosphorylation of Smad2 and Smad3 (the first

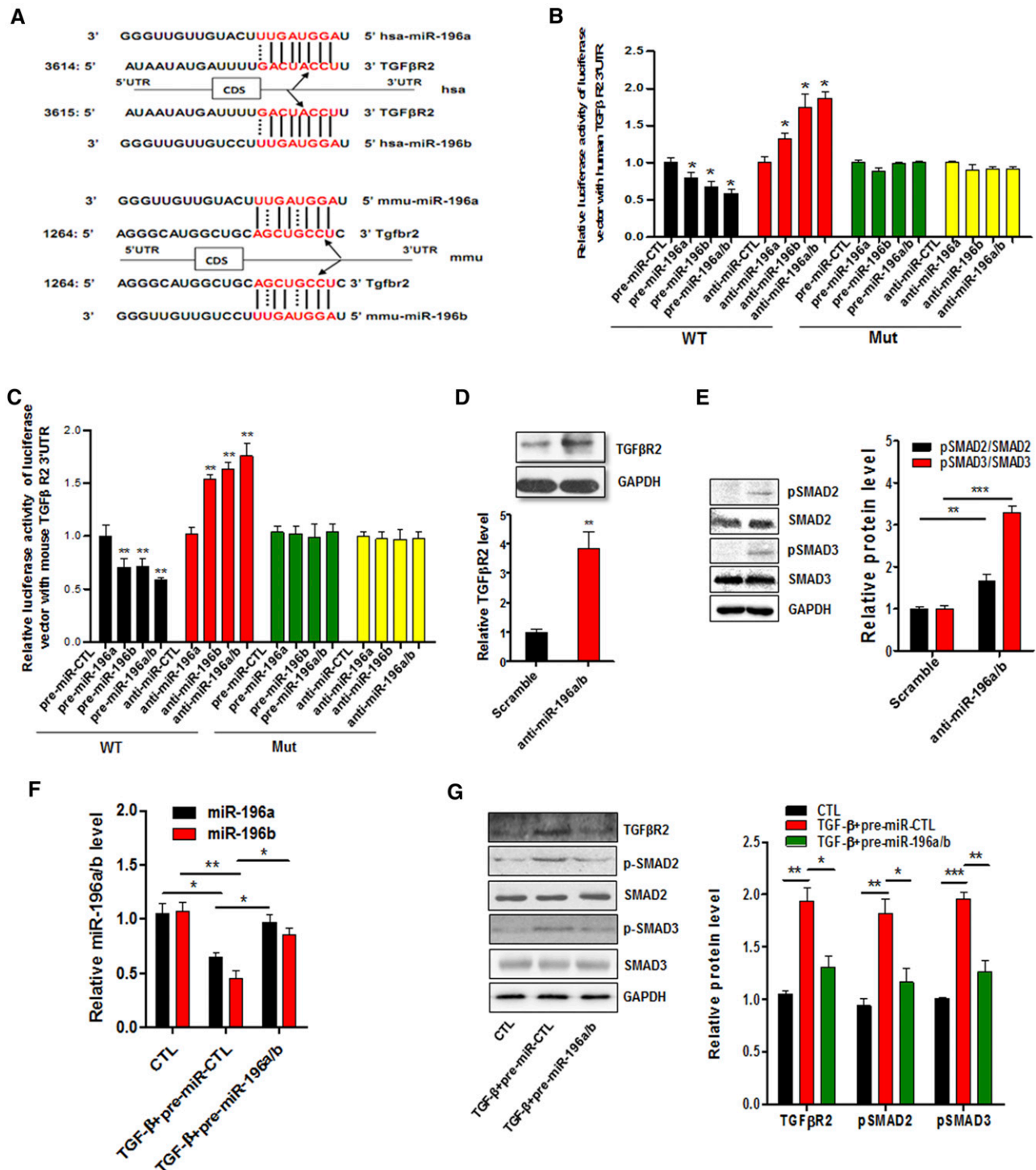


**Figure 6.** Identification of TGFβR2 as a common target gene of miR-196a and miR-196b. (A) Schematic diagram of TGFβR2 3'-UTR as a putative target for miR-196a and miR-196b. The seed-recognizing sites in the TGFβR2 3'-UTR by miR-196a and miR-196b are indicated in red. (B) Relative luciferase activity in HK2 cells that are cotransfected with plasmids containing firefly luciferase and wild-type (WT) or mutant (Mut) human TGFβR2 3'-UTR and pre-miR-196a, pre-miR-196b, miR-196a antagomir (anti-miR-196a), miR-196b antagomir (anti-miR-196b), pre-miR-196a and pre-miR-196b (pre-miR-196a/b), miR-196a and miR-196b antagomir (anti-miR-196a/b), or respective control oligonucleotides (pre-miR-CTL and anti-miR-CTL). (C) Relative luciferase activity in 293T cells cotransfected with plasmids containing firefly luciferase and wild-type or mutant mouse TGFβR2 3'-UTR and pre-miR-196a, pre-miR-196b, miR-196a antagomir, miR-196b antagomir, pre-miR-196a and pre-miR-196b, miR-196a and miR-196b antagomirs, or respective control oligonucleotides. (D) Western blot analysis of TGFβR2 levels in HK2 cells transfected with scrambled oligonucleotide or miR-196a and



step in signal transduction),<sup>36</sup> we next examined the effect of knocking down miR-196a and miR-196b on the level of phosphorylated SMAD2 and SMAD3 in HK2 cells. As shown in Figure 6E, depletion of both miR-196a and miR-196b in HK2 cells strongly increased the levels of phosphorylated SMAD3, as well as the levels of phosphorylated SMAD2, albeit at a lesser degree, compared with the cells transfected with control oligonucleotides. Our results confirmed that both miR-196a and miR-196b downregulate TGF $\beta$ R2 and TGF- $\beta$  signaling activity in HK2 cells. To further test the suppressive effect of miR-196a and miR-196b on the level of TGF $\beta$ R2 and TGF- $\beta$ /TGF $\beta$ R2-initiated signaling, we used mouse primary cultured tubular epithelial cells. In this experiment, 4 ng/ml TGF- $\beta$  was added to induce fibrosis in primary cultured tubular epithelial cells. As shown in Figure 6F, TGF- $\beta$  significantly reduced the expression of miR-196a and miR-196b in primary cultured mouse tubular epithelial cells after 24 hours' incubation. However, transfection with miR-196a/b-expressing plasmids completely rescued the reduction of miR-196a and miR-196b induced by TGF- $\beta$ , and thus suppressed TGF $\beta$ R2 expression as well as the TGF- $\beta$ /TGF $\beta$ R2-mediated signaling downstream (Figure 6G).

Next, we determined whether renal miR-196a and miR-196b are also downregulated in patients with renal fibrosis. For this experiment, we analyzed the renal biopsy tissue samples from three patients with diabetic nephropathy and renal fibrosis and three normal controls (Table 1). Normal control kidney tissues were obtained from nondiseased portions of nephrectomy specimens of patients who had undergone surgery to remove localized renal tumors. A Masson trichrome staining assay confirmed severe renal fibrosis in the kidneys from the patients compared, with a lesser degree of renal fibrosis in normal controls (Figure 7, A and B). As shown by qRT-PCR assay in Figure 7C, renal levels of miR-196a and miR-196b in patients with renal fibrosis were significantly reduced compared with those in normal controls. Immunohistochemical staining further indicated that the level of TGF $\beta$ R2 in the kidneys from patients with renal fibrosis was higher than in those from normal controls (Figure 7D).

#### miR-196a/b Attenuate UUO-Induced Mouse Renal Fibrosis via Suppression of the Activation of the TGF- $\beta$ Signaling Pathway

We next examined the effect of miR-196a and miR-196b in mice on the expression of TGF $\beta$ R2, the activation of the TGF- $\beta$  signaling pathway, and the expression of the fibrotic proteins

**Table 1.** Information on the control subjects and patients with renal fibrosis enrolled in the study

Clinical Feature	Control	Fibrosis
Agea (years)	45.67 $\pm$ 4.58	48.2 $\pm$ 3.96
Gender (male/female)	2/1	2/1
Proteinuria <sup>a</sup> (g/24 h)	0.32 $\pm$ 0.12	5.632 $\pm$ 3.13 <sup>b</sup>
Serum creatinine <sup>a</sup> (mg/dl)	0.79 $\pm$ 0.15	1.675 $\pm$ 0.76 <sup>b</sup>
BUN <sup>c</sup> (mmol/L)	10.12 (8.31, 12.01)	24.65 (19.1, 31.2) <sup>b</sup>
eGFR <sup>a</sup> (ml/min per 1.73 m <sup>2</sup> )	110.17 $\pm$ 10.61	52.737 $\pm$ 21.69 <sup>b</sup>

<sup>a</sup>Mean $\pm$ SD.

<sup>b</sup>P<0.01.

<sup>c</sup>Median (25th percentile, 75th percentile).

COL1 and  $\alpha$ -SMA. As shown in Figure 8, A and B, we observed only a minimal level of TGF $\beta$ R2 and little accumulation of COL1 and  $\alpha$ -SMA in the kidneys of untreated control mice. In contrast, in kidney tissue sections of UUO mice (assessed on day 7 after UUO treatment), immune-labeling of TGF $\beta$ R2 was significantly increased and we detected a substantial amount of COL1 and  $\alpha$ -SMA accumulation. However, increasing the level of renal miR-196a and miR-196b expression through delivery of miR-196a/b-expressing plasmids before the UUO procedure led to a strong reduction in the immune-labeling of TGF $\beta$ R2 and the accumulation of COL1 and  $\alpha$ -SMA in mouse kidneys. We confirmed the suppressive effects of miR-196a/b on protein expression of TGF $\beta$ R2 and fibrotic markers by Western blot analysis using freshly isolated mouse kidney tissues (Figure 8, C and D). Clearly, the levels of TGF $\beta$ R2, p-SMAD2, p-SMAD3, COL1, and  $\alpha$ -SMA in mouse kidneys were increased in the UUO group. In contrast, in those mice transfected with miR-196a/b-expressing plasmids before (Figure 8C) or shortly after (Figure 8D) the UUO procedure, the levels of TGF $\beta$ R2, p-SMAD2, p-SMAD3, COL1, and  $\alpha$ -SMA remained at control levels. Mice administered miR-196a/b antagonists after the UUO procedure, however, displayed a significantly increased expression of TGF $\beta$ R2 and the accumulation of COL1 and  $\alpha$ -SMA in their kidneys compared with UUO mice administered scramble oligonucleotides (Figure 8, E and F). Western blot analysis confirmed that treatment with miR-196a/b antagonists further enhanced the UUO-induced TGF $\beta$ R2, p-SMAD2, p-SMAD3, COL1, and  $\alpha$ -SMA expression in UUO mouse kidneys (Figure 8G). Collectively, our results show that miR-196a and miR-196b can attenuate UUO-induced mouse renal fibrosis *via* reducing the level of TGF $\beta$ R2, thereby abrogating profibrotic TGF- $\beta$ -Smad signaling.

miR-196b antagonist. (E) Western blot analysis of p-SMAD2/SMAD2, p-SMAD3/SMAD3 in HK2 cells cotransfected with miR-196a/b antagonists. (F) Reduction of miR-196a and miR-196b in primary cultured mouse tubular epithelial cells induced by TGF- $\beta$  (4 ng/ml, 24 hours). (G) Overexpression of miR-196a/b reduced the expression of TGF $\beta$ R2 and the downstream signaling pathways induced by TGF- $\beta$  in primary cultured mouse tubular epithelial cells. Results are presented as mean $\pm$ SEM from three independent experiments. \*P<0.05; \*\*P<0.01; \*\*\*P<0.001.

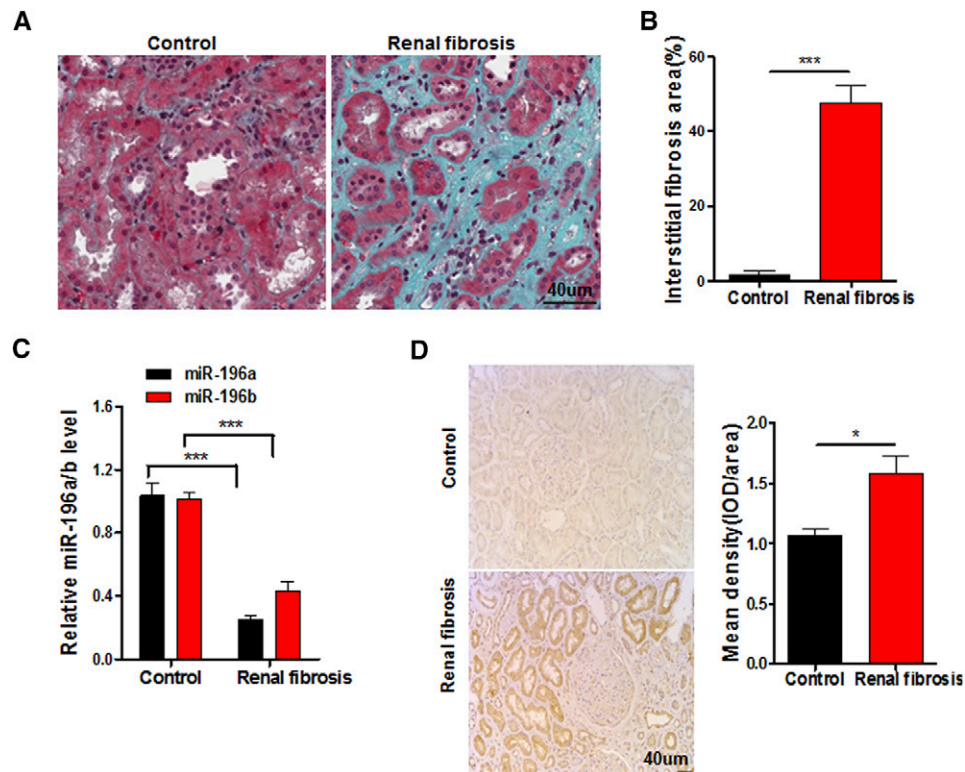


**Figure 7.** Renal miR-196a and miR-196b are significantly downregulated in patients with renal fibrosis. (A) Representative images of Masson trichrome staining of kidneys of patients with renal fibrosis and normal controls (Control). Magnification,  $\times 400$ . (B) Quantitative analysis of tubular interstitial fibrosis from Masson trichrome staining. (C) Levels of miR-196a and miR-196b in the microdissected tubular interstitial sections from three patients with renal fibrosis and three control subjects assayed by qRT-PCR. (D) Representative immunohistochemical staining images of TGF $\beta$ R2 in the microdissected tubular interstitial sections from patients with renal fibrosis and control subjects. Magnification,  $\times 200$ . Right histogram represents semiquantitative analysis of TGF $\beta$ R2 through measuring the signal density in five or six randomly selected fields. Results are presented as mean  $\pm$  SEM from three independent experiments. \* $P < 0.05$ ; \*\*\* $P < 0.001$ .

## DISCUSSION

The role of miRNAs in controlling the expression of proteins in the tissues of various organs has been the focus of an emerging body of research. Emerging evidence suggests that each organ expresses a unique panel of miRNAs and these miRNAs play an essential role in maintaining homeostasis.<sup>5,37</sup> Therefore, identification of kidney-enriched miRNAs and exploring their biologic function are critical for understanding the role of miRNAs in renal development and pathologic processes. Using Solexa deep sequencing, we performed an unbiased assessment of whole-genome miRNA expression in various mouse organs and identified miR-196a and miR-196b as the kidney-enriched miRNAs. The predominance of miR-196a/b in kidney was confirmed by TaqMan probe-based qRT-PCR and *in situ* hybridization techniques using both mouse and human samples.

The possibility of selective expression of miRNA in different organs from human, mouse, rat and zebra fish has been explored previously by different investigators,<sup>5,37,38</sup> and the results suggest that particular organs indeed exhibit unique miRNA expression profiles. For example, miR-1 and miR-

133 are enriched in heart, and miR-9 and miR-122 are predominantly expressed in brain and liver, respectively.<sup>5,37</sup> The tissue-enriched expression pattern of miRNAs in animals suggests a critical role of such miRNAs in maintaining the homeostasis of particular organs. For instance, miR-122 is important in maintaining a healthy liver structure and function by suppressing the progression of hepatocellular carcinoma, whereas a decrease in the miR-122 expression level positively correlates with poor prognosis.<sup>7,39</sup> In addition, miR-122 is also a key regulator of cholesterol and fatty-acid metabolism in the adult liver.<sup>40</sup> The miRNAs that predominantly express in cardiac and skeletal muscle tissue, such as miR-1 and miR-133, also play an important role in modulating muscle proliferation and differentiation.<sup>38</sup> Recent studies have also shown that certain miRNAs are enriched in human and mouse kidney.<sup>5,8,9,37,41,42</sup> It is worth noting that, through an approach of cloning and sequencing  $>250$  small RNA libraries from different cell types and tissues, Landgraf *et al.*<sup>8</sup> have observed that a panel of miRNAs, including miR-196a/b, was enriched in mouse kidney. In this study, by comparing the genome-wide expression profile of miRNA in various mouse

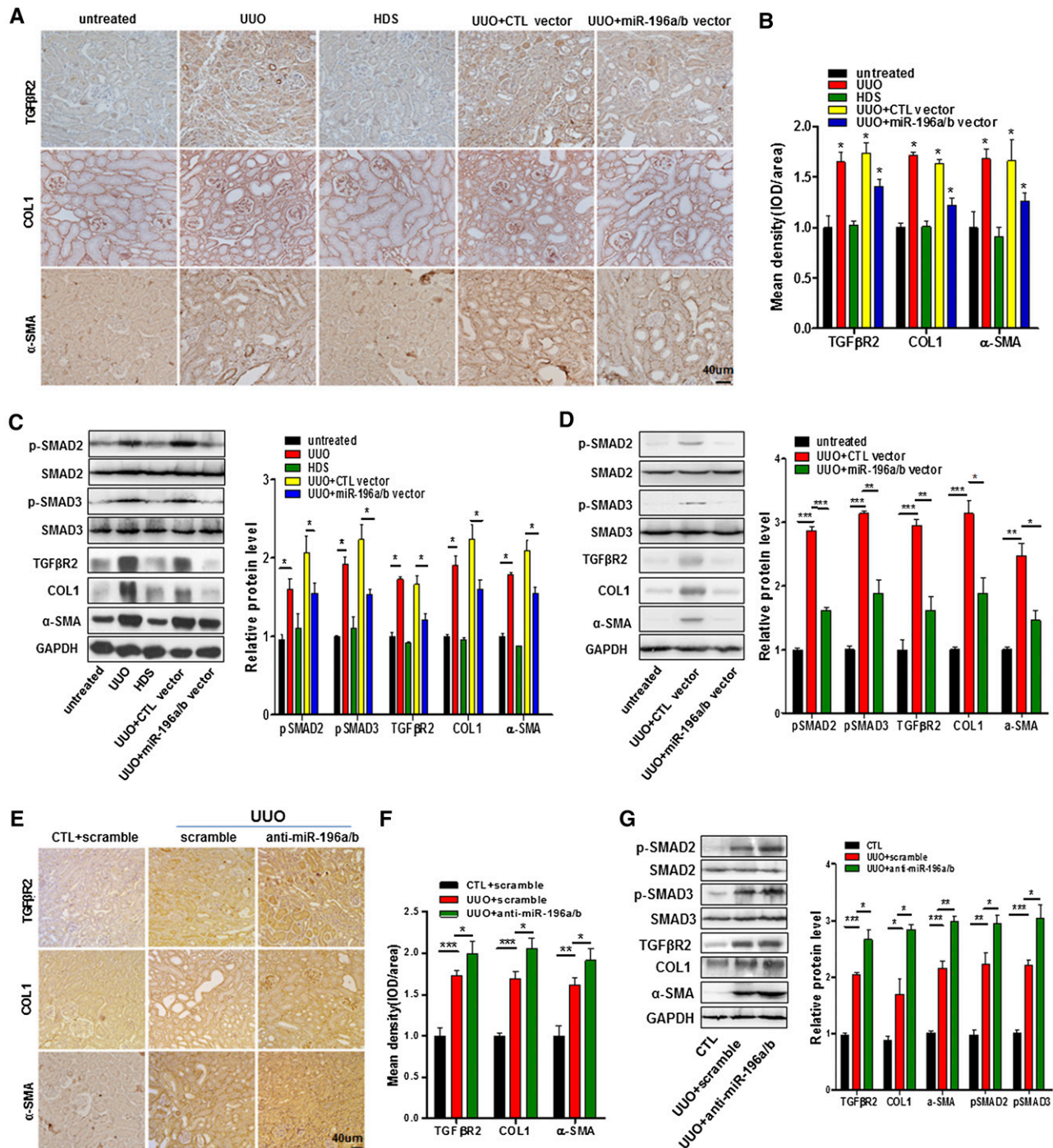


**Figure 8.** MiR-196a and miR-196b alleviate renal fibrosis in UUO mice through inhibiting activation of the TGF- $\beta$  signaling pathway. (A) Representative immunohistochemical staining of TGF $\beta$ R2, COL1, and  $\alpha$ -SMA in kidneys of untreated and UUO mice (7 days post-UUO) injected with miR-196a/b-expressing vector or control vector before the UUO procedure. Magnification,  $\times 200$ . (B) Quantitative analysis of TGF $\beta$ R2, COL1, and  $\alpha$ -SMA levels in kidneys. (C) Representative Western blots of TGF $\beta$ R2, p-SMAD2/SMAD2, p-SMAD3/SMAD3, COL1, and  $\alpha$ -SMA in the kidneys of untreated and UUO mice (7 days post-UUO) that were injected with miR-196a/b-expressing vector or control vector. Right histogram represents quantitative analysis of protein level. (D) Representative Western blots of TGF $\beta$ R2, p-SMAD2/SMAD2, p-SMAD3/SMAD3, COL1, and  $\alpha$ -SMA in the kidneys of untreated and UUO mice injected with miR-196a/b-expressing vector or control vector after UUO treatment. Right histogram represents quantitative analysis of protein level. (E) Representative immunohistochemical staining images of TGF $\beta$ R2, COL1, and  $\alpha$ -SMA in kidneys of control and UUO mice (7 days post-UUO) injected with miR-196a/b antagonirs or control oligonucleotides after UUO treatment. (F) Quantitative analysis of TGF $\beta$ R2, COL1, and  $\alpha$ -SMA levels. (G) Representative Western blots of TGF $\beta$ R2, p-SMAD2/SMAD2, p-SMAD3/SMAD3, COL1, and  $\alpha$ -SMA in



organs, our results confirmed that miR-196a and miR-196b are predominantly expressed in kidney, with 74.37% and 73.19% of total mouse miR-196a and miR-196b, respectively, being distributed in the kidneys.

We sought to explore how miRNA might be relevant to the disease process of renal fibrosis. Renal fibrosis is an inevitable consequence of many CKDs and ultimately leads to end stage renal failure. Among the diverse causative factors, it is widely accepted that TGF- $\beta$  and its downstream Smad signaling play an essential role in inducing renal fibrosis. Emerging evidence has demonstrated that many miRNAs participating in renal fibrosis modulation are regulated by TGF- $\beta$ .<sup>24–28,43,44</sup> TGF- $\beta$  has been found to be able to upregulate miR-21, miR-192, miR-377, miR-143, and miR-150, but downregulate miR-29 and miR-200 families, in patients or animal models with renal fibrosis.<sup>24–28,43,44</sup> In this study, our results indicated that kidney miR-196a and miR-196b are significantly decreased during UUO-induced renal fibrosis, in which TGF- $\beta$ –Smad signaling plays a critical role. However, it remains unknown whether expression of miR-196a and miR-196b is directly modulated by TGF- $\beta$  *in vivo*. Our results showed that the pathologic changes can be improved by overexpressing miR-196a/b in the kidney before or after the UUO procedure. We identified TGF $\beta$ 2, an important receptor for initiating profibrotic TGF- $\beta$ –Smad signaling, as a common target of miR-196a and miR-196b in both humans and mice. An *in vitro* study using a firefly luciferase reporter plasmid containing the predicted TGF $\beta$ 2 target gene sequences showed that TGF $\beta$ 2 is a direct target of miR-196a/b in humans and mice. Consistent with miR-196a/b targeting mRNA of TGF $\beta$ 2, we showed that miR-196a/b inhibitors increased the expression of TGF $\beta$ 2. To further determine whether miR-196a/b–induced TGF $\beta$ 2 downregulation affected pathways downstream of TGF- $\beta$ , we transfected HK2 cells with miR-196a/b inhibitors and found that the addition of the inhibitors increased SMAD2 and SMAD3 phosphorylation, indicating that TGF- $\beta$  signaling had occurred. An *ex vivo* study showed the expression of miR-196a and miR-196b in primary cultured mouse tubular epithelial cells was reduced by TGF- $\beta$  treatment, and rescuing the reduction of miR-196a and miR-196b significantly inhibited the expression of TGF $\beta$ 2 and downstream SMAD signal induced by TGF- $\beta$ . A further study on the relevance of miR196a/b and TGF $\beta$ 2 in human renal fibrosis confirmed the role of miR-196a and miR-196b in kidney, suggesting that miR-196a/b are important mediators in renal fibrosis and may serve as potential therapeutic targets to prevent or treat renal fibrosis.

TGF- $\beta$  evokes diverse cellular responses, leading to different pathophysiologic consequences including renal fibrosis.

After binding to cell-surface receptors, particularly TGF $\beta$ 2, TGF- $\beta$  initiated TGF- $\beta$ –Smad signaling downstream. In both experimental and human kidney diseases, such as diabetic nephropathy<sup>45,46</sup> and obstructive kidney disease,<sup>18</sup> Smad3 is considered to be a critical mediator of TGF- $\beta$ –Smad signaling in fibrosis. The importance of TGF $\beta$ 2 in TGF- $\beta$  signaling has been demonstrated in mouse knockout experiments.<sup>47</sup> A recent study demonstrated that the expression level of TGF $\beta$ 2 is directly correlated with TGF- $\beta$  response, and plays an important role in promoting renal fibrosis after injury.<sup>48–50</sup> Active TGF- $\beta$  exerts its biologic and pathologic activities *via* Smad-dependent and Smad-independent signaling pathways,<sup>22</sup> and the Smad-dependent mechanism has been considered to be a major pathway in many pathophysiologic processes of kidney disease.<sup>19,51–53</sup> Therefore, downregulation of TGF $\beta$ 2 expression by miR-196a/b might improve renal fibrosis by blocking TGF- $\beta$  signal transduction at the very early stage. Our results showed that TGF $\beta$ 2, Smad2, and Smad3 were significantly upregulated in the UUO 7-day group compared with the control group. The downregulation of miR-196a/b in the kidneys of UUO and the primary cultured mouse tubular epithelial cells stimulated by TGF- $\beta$  observed in this study suggests that TGF- $\beta$  may perform a role in regulating the expression of miR-196a/b.

In conclusion, this study has identified that miR-196a and miR-196b are predominantly expressed in the kidney. Our results provide the first evidence that miR-196a and miR-196b play an inhibitory role in the progress of renal fibrosis through downregulation of TGF $\beta$ 2, and that maintaining renal miR-196a and miR-196b levels *via* delivery of a miR-196a/b–expressing vector is a potential therapeutic strategy for renal fibrosis.

## CONCISE METHODS

### Solexa Deep Sequencing

We freshly isolated mouse organs, including heart, liver, kidney, stomach, spleen, cerebrum, cerebellum, small intestine, lung, pancreas, ovary, esophagus, uterus, and colon, from C57/B6 female mice (8 weeks, 22–25 g) after euthanization followed by whole-body saline perfusion. We extracted total RNA from each organ and analyzed whole-genome miRNA expression in various mouse organs by Solexa deep sequencing as previously described.<sup>54</sup> Briefly, we purified small RNA molecules <30 bases by PAGE and then ligated a pair of adaptors (Illumina, San Diego, CA) to the 5' and 3' ends of the purified small RNAs. We amplified the adaptor-ligated small RNA molecules using the adaptor primers for 17 cycles, and isolated the fragments of around 90 bp (small RNA and adaptors) from the agarose gel. Then we used the generated cDNA library directly for sequencing analysis

kidneys of control and UUO mice (7 days post-UUO) injected with miR-196a/b antagomirs or control oligonucleotides after UUO treatment. Right histogram represents quantitative analysis of protein levels. We normalized protein levels to the level of GAPDH. Results are presented as mean  $\pm$  SEM from three independent experiments. \* $P$ <0.05; \*\* $P$ <0.01; \*\*\* $P$ <0.001.

using the Illumina Genome Analyzer, according to the manufacturer's instructions. For quality control, we removed the sequences with low quality scores. After trimming the 3' adapter, we removed sequences with length below 16 bp, 5' adapter contamination, and poly(A). Then we aligned the clean reads to the pre-miRNA sequences. Sequenced reads with no more than two mismatches and two shifts we identified as one miRNA. We normalized miRNA reads as miRNA reads  $\times 1,000,000/\text{total reads}$ . We calculated the percentages of different miRNAs in tissues as miRNA reads in each tissue/total miRNA reads in all 14 mouse tissues.

### Cell Culture and Human Kidney Tissue Samples

We procured human renal proximal tubular epithelial (HK2) cells from the American Type Culture Collection and maintained them in DMEM/F12 medium supplemented with 10% FBS and antibiotics. For primary tubular cell culture, we isolated cortical fragments of kidneys from male C57/BL6-mice (8–10 weeks old) under sterile conditions. We dissected renal cortices into pieces (1 mm) and transferred these to collagenase solution and digested them for 30 minutes at 37°C. After the digestion, we filtered the supernatant through 80- $\mu\text{m}$  nylon sieves. The larger fragments in the sieve we resuspended; centrifuged for 5 minutes at 170 $\times g$ ; washed; resuspended in DMEM/F12 supplemented with heat-inactivated 10% FCS, 50 nmol/L hydrocortisone, 100 $\times$  ITS (Sigma-Aldrich, St. Louis, MO), and 100 $\times$  non-essential amino acids; and then seeded onto collagen-coated culture dishes for 48 hours at 37°C and 5% CO<sub>2</sub>. We then replaced the medium every 2 days. We obtained normal kidney tissues from normal portions of nephrectomy specimens of patients who had undergone surgery to remove localized renal tumors.

### Microdissection of Glomerulus and Tubular Interstitium

We obtained the kidney samples used to determine miR-196a/b expression in glomerulus or tubular interstitium from patients with renal fibrosis or normal controls. We obtained the control renal tissues from the intact pole of kidneys that had been removed for single circumscribed tumors, and verified the tissue's normality by light microscopy. We cut kidney tissues from each normal control subject into five sections (6  $\mu\text{m}$  thick) and mounted them on Leica frame slides (Leica FrameSlides PPS-Membrane, Leica Microsystems, Buffalo Grove, IL). After deparaffinizing tissue sections using xylene and dehydrating them in ethanol, we isolated glomeruli by laser capture using a Leica LMD System. In each section, we randomly sampled 20–25 fields of view (with three to eight glomerular cross sections per field) at a magnification of  $\times 100$ . We microdissected and collected the glomerular cross sections presented in these fields, and collected the rest of the sections (the renal tubules and interstitial) in 1.5-ml centrifuge tubes for further assay.

### RNA Isolation and Quantitative RT-PCR Assays

We extracted total RNA from cultured cells and kidney tissues with TRIzol Reagent (Invitrogen, Carlsbad, CA), according to the manufacturer's instructions. We used gene-specific TaqMan miRNA Assay Probes (Applied Biosystems, Foster City, CA) to assay the miR-196a/b quantification. Briefly, we reverse-transcribed 1  $\mu\text{g}$  of total RNA to cDNA using AMV reverse transcription (Takara, Kyoto,

Japan) and a stem-loop RT primer (Applied Biosystems). We performed real-time PCR using a TaqMan PCR kit on an Applied Biosystems 7900HT Sequence Detection System. We ran all reactions, including no-template controls, in triplicate. After the reactions, we determined the threshold cycles ( $C_T$ ) values using fixed-threshold settings. We normalized the miRNA expression in cells and tissues to U6 snRNA.

### Luciferase Reporter Assay

We amplified the human and mouse TGF $\beta$ R2 fragments containing putative binding sites located in the human TGF $\beta$ R2 3'-UTR by PCR using human genomic DNA as a template. We inserted the PCR products into the p-MIR-REPORT plasmid (Ambion), and confirmed efficient insertion by sequencing. To test the binding specificity, we mutated the sequences in the human and mouse TGF $\beta$ R2 3'UTR that interact with the miR-196a/b seed sequence (human, from GACUACCU to CUGAUGGA; mouse, from AGCUGCCU to UCGACGGA). For the luciferase reporter assay, we cultured cells in six-well plates, and transfected each well with 1 mg firefly luciferase reporter plasmid, 1 mg  $\beta$ -galactosidase ( $\beta$ -gal) expression plasmid (Ambion), and cotransfected with equal amounts (100 pmol) of pre-miR-196a/b, anti-miR-196a/b, or scrambled negative control RNA using Lipofectamine 2000. Luciferase activities we measured at 24 hours after transfection using luciferase assay kits (Promega).

### Animals and Obstructive Kidney Disease Model

We performed all animal care and experiments according to the guidelines of the Institutional Animal Care and Use Committee at Nanjing University. We obtained the male C57BL/6J mice (8 weeks, 22–25 g) used in this study from the Model Animal Research Center of Nanjing University (Nanjing, China). We performed UUO model surgery as previously described.<sup>55</sup> Briefly, we anesthetized mice with intraperitoneal injection of pentobarbital (50 mg/kg). We then divided the mice into two groups: the UUO group and the sham operation group. In the UUO group, we exposed the left ureter *via* a midline incision and ligated it twice 15 mm below the renal pelvis with 4–0 silk. The sham operation group we handled in a similar manner, but without ureteral ligation. In order to express exogenous miR-196a/b in the kidney of mice, we administered GFP-labeled miR-196a/b-expressing plasmid DNA (Genscript, Nanjing, China) to the mice using a previously described hydrodynamic-based gene-transfer technique.<sup>56</sup> Briefly, we mixed miR-196a/b-expressing plasmids (20  $\mu\text{g}$  each) into approximately 2.6 ml (15.4  $\mu\text{g}/\text{ml}$ ) of TransIT-EE Hydrodynamic Delivery Solution (Mirus). To deplete miR-196a and miR-196b, we mixed 2 nM of each miR-196a and miR-196b antagomir (Ribobio, Guangzhou, China) into 2.6 ml of TransIT-EE Hydrodynamic Delivery Solution. Then we injected the mixture into mice *via* the tail vein in <5 seconds. We harvested obstructed kidneys at 7 days after UUO for Western blot, real-time PCR, histology examination, and immunohistochemistry.

### Histology and Immunohistochemistry

We embedded tissues in paraffin. We deparaffinized 2- $\mu\text{m}$  paraffin kidney sections, and rehydrated and washed them in distilled water. To evaluate kidney histologic changes such as the degree of tubular atrophy and interstitial fibrosis, we processed sections for Masson

trichrome staining. We performed immunohistochemistry in paraffin sections using a microwave-based antigen retrieval technique.<sup>57</sup> After blocking the slides with 5% normal goat serum, we incubated them overnight at 4°C with primary antibodies raised against TGF $\beta$ R2 (Cell Signaling Technology, Danvers, MA), CD11b,  $\alpha$ -SMA, and collagen I (COL1) (Abcam plc, Cambridge, UK). We developed immunohistochemical staining in tissue sections with DAB after 30 minutes, and then counter-stained them with hematoxylin. We quantified percentages of positive staining area using Image-Pro plus 6.0 software.

### Morphometric Analysis of the Interstitial Fibrosis

We determined the area of the fibrotic lesion of the renal interstitium in sections stained using the Masson trichrome method to stain collagen fibers (in light blue) in the tubular basement membrane, glomeruli, and interstitial space. We highlighted the fibrotic areas in the interstitium on digitized images using a computer-aided manipulator (microscope, Leitz DM IRB; software, Quantimet 500+; Leica Microsystems). Under high-power magnification (400 $\times$ ), we selected ten nonoverlapping fields at random and an observer unaware of the experimental protocol analyzed the fields. We calculated the fibrotic area relative to the total area of the field as a percentage.

### Western Blot

We analyzed the levels of TGF $\beta$ R2, SMAD2, p-SMAD2, SMAD3, p-SMAD3, COL1, and  $\alpha$ -SMA by Western blot using primary antibodies against TGF $\beta$ R2, SMAD2, p-SMAD2, SMAD3, p-SMAD3, COL1,  $\alpha$ -SMA, and GAPDH (Santa Cruz Biotechnology, Santa Cruz, CA), respectively. We normalized the protein levels against that of GAPDH.

### In Situ Hybridization

We performed *in situ* hybridization for miR-196a and miR-196b using double digoxigenin-labeled LNA miRCURY probes (Exiqon). A scrambled probe served as a negative control and U6 served as the positive control. Briefly, we euthanized mice and embedded the kidneys in paraffin. Then we prepared 5- $\mu$ m-thick sections of FFPE. The tissue we deparaffinized by sequential washes with xylene, 70%, 95% and 100% ethanol, and PBS. We treated the sections with 5 mg/ml proteinase K for 10 minutes at room temperature. We performed hybridization with a probe concentration of 50 nM in hybridization buffer overnight at 50°C. After a series of posthybridization washes, we blocked the sections with blocking buffer and then incubated them with anti-digoxigenin-alkaline phosphatase in blocking buffer for 1 hour. We washed the sections repeatedly in PBS and 0.1% Tween 20, labeled with NBT/BCIP for 2 hours at 30°C, followed by double staining with fast red to illuminate nuclei. We mounted the sections in glycerol and viewed them under phase-contrast microscopy.

### Statistical Analyses

Each experiment is representative of at least three independent experiments. We performed real-time qRT-PCR assays in triplicate. All data are expressed as mean  $\pm$  SEM. We considered differences between groups to be statistically significant at  $P < 0.05$ , analyzed using the *t* test. We analyzed more than two group differences by ANOVA.

Nonparametric variables are expressed as the median (range) values and we compared these using the Kruskal–Wallis test.

### ACKNOWLEDGMENTS

This work was supported by grants from the National Basic Research Program of China (973 Program, no. 2012CB517603), the National Natural Science Foundation of China (no. 31301061), the Natural Science Foundation of Jiangsu Province (no. BK20130564), and the Specialized Research Fund for the Doctoral Program of Higher Education (no. 20130091120037).

### DISCLOSURES

None.

### REFERENCES

1. Pasquinelli AE: MicroRNAs and their targets: recognition, regulation and an emerging reciprocal relationship. *Nat Rev Genet* 13: 271–282, 2012
2. Peláez N, Carthew RW: Biological robustness and the role of microRNAs: a network perspective. *Curr Top Dev Biol* 99: 237–255, 2012
3. Kloosterman WP, Plasterk RH: The diverse functions of microRNAs in animal development and disease. *Dev Cell* 11: 441–450, 2006
4. Shivdasani RA: MicroRNAs: regulators of gene expression and cell differentiation. *Blood* 108: 3646–3653, 2006
5. Lagos-Quintana M, Rauhut R, Yalcin A, Meyer J, Lendeckel W, Tuschl T: Identification of tissue-specific microRNAs from mouse. *Curr Biol* 12: 735–739, 2002
6. Jopling C: Liver-specific microRNA-122: Biogenesis and function. *RNA Biol* 9: 137–142, 2012
7. Coulouarn C, Factor VM, Andersen JB, Durkin ME, Thorgerirsson SS: Loss of miR-122 expression in liver cancer correlates with suppression of the hepatic phenotype and gain of metastatic properties. *Oncogene* 28: 3526–3536, 2009
8. Landgraf P, Rusu M, Sheridan R, Sewer A, Iovino N, Aravin A, Pfeffer S, Rice A, Kamphorst AO, Landthaler M, Lin C, Socci ND, Hermida L, Fulci V, Chiaretti S, Foà R, Schliwka J, Fuchs U, Novosel A, Müller RU, Schermer B, Bissels U, Inman J, Phan Q, Chien M, Weir DB, Choksi R, De Vita G, Frezzetti D, Trompeter H, Hornung V, Teng G, Hartmann G, Palkovits M, Di Lauro R, Wernet P, Macino G, Rogler CE, Nagle JW, Ju J, Papavasiliou FN, Benzing T, Lichter P, Tam W, Brownstein MJ, Bosio A, Borkhardt A, Russo JJ, Sander C, Zavolan M, Tuschl T: A mammalian microRNA expression atlas based on small RNA library sequencing. *Cell* 129: 1401–1414, 2007
9. Sun Y, Koo S, White N, Peralta E, Esau C, Dean NM, Perera RJ: Development of a micro-array to detect human and mouse microRNAs and characterization of expression in human organs. *Nucleic Acids Res* 32: e188, 2004
10. Remuzzi G, Bertani T: Pathophysiology of progressive nephropathies. *N Engl J Med* 339: 1448–1456, 1998
11. Müller GA, Zeisberg M, Strutz F: The importance of tubulointerstitial damage in progressive renal disease. *Nephrol Dial Transplant* 15[Suppl 6]: 76–77, 2000
12. Iwano M, Neilson EG: Mechanisms of tubulointerstitial fibrosis. *Curr Opin Nephrol Hypertens* 13: 279–284, 2004
13. Grande MT, López-Novoa JM: Fibroblast activation and myofibroblast generation in obstructive nephropathy. *Nat Rev Nephrol* 5: 319–328, 2009



14. Boor P, Ostendorf T, Floege J: Renal fibrosis: novel insights into mechanisms and therapeutic targets. *Nat Rev Nephrol* 6: 643–656, 2010
15. Zeisberg M, Neilson EG: Mechanisms of tubulointerstitial fibrosis. *J Am Soc Nephrol* 21: 1819–1834, 2010
16. Bohle A, Müller GA, Wehrmann M, Mackensen-Haen S, Xiao JC: Pathogenesis of chronic renal failure in the primary glomerulopathies, renal vasculopathies, and chronic interstitial nephritides. *Kidney Int Suppl* 54: S2–S9, 1996
17. Böttinger EP, Bitzer M: TGF- $\beta$  signaling in renal disease. *J Am Soc Nephrol* 13: 2600–2610, 2002
18. Sato M, Muragaki Y, Saika S, Roberts AB, Ooshima A: Targeted disruption of TGF- $\beta$ 1/Smad3 signaling protects against renal tubulointerstitial fibrosis induced by unilateral ureteral obstruction. *J Clin Invest* 112: 1486–1494, 2003
19. Wang W, Koka V, Lan HY: Transforming growth factor- $\beta$  and Smad signalling in kidney diseases. *Nephrology (Carlton)* 10: 48–56, 2005
20. Fogo AB: Mechanisms of progression of chronic kidney disease. *Pediatr Nephrol* 22: 2011–2022, 2007
21. Massagué J: TGF- $\beta$  signal transduction. *Annu Rev Biochem* 67: 753–791, 1998
22. Derynck R, Zhang YE: Smad-dependent and Smad-independent pathways in TGF- $\beta$  family signalling. *Nature* 425: 577–584, 2003
23. Kato M, Zhang J, Wang M, Lanting L, Yuan H, Rossi JJ, Natarajan R: MicroRNA-192 in diabetic kidney glomeruli and its function in TGF- $\beta$ -induced collagen expression via inhibition of E-box repressors. *Proc Natl Acad Sci U S A* 104: 3432–3437, 2007
24. Wang Q, Wang Y, Minto AW, Wang J, Shi Q, Li X, Quigg RJ: MicroRNA-377 is up-regulated and can lead to increased fibronectin production in diabetic nephropathy. *FASEB J* 22: 4126–4135, 2008
25. Putta S, Lanting L, Sun G, Lawson G, Kato M, Natarajan R: Inhibiting microRNA-192 ameliorates renal fibrosis in diabetic nephropathy. *J Am Soc Nephrol* 23: 458–469, 2012
26. Chung AC, Huang XR, Meng X, Lan HY: miR-192 mediates TGF- $\beta$ /Smad3-driven renal fibrosis. *J Am Soc Nephrol* 21: 1317–1325, 2010
27. Wang B, Komers R, Carew R, Winbanks CE, Xu B, Herman-Edelstein M, Koh P, Thomas M, Jandeleit-Dahm K, Gregorevic P, Cooper ME, Kantharidis P: Suppression of microRNA-29 expression by TGF- $\beta$ 1 promotes collagen expression and renal fibrosis. *J Am Soc Nephrol* 23: 252–265, 2012
28. Xiong M, Jiang L, Zhou Y, Qiu W, Fang L, Tan R, Wen P, Yang J: The miR-200 family regulates TGF- $\beta$ 1-induced renal tubular epithelial to mesenchymal transition through Smad pathway by targeting ZEB1 and ZEB2 expression. *Am J Physiol Renal Physiol* 302: F369–F379, 2012
29. Wu J, Zheng C, Fan Y, Zeng C, Chen Z, Qin W, Zhang C, Zhang W, Wang X, Zhu X, Zhang M, Zen K, Liu Z: Downregulation of microRNA-30 facilitates podocyte injury and is prevented by glucocorticoids. *J Am Soc Nephrol* 25: 92–104, 2014
30. Shi S, Yu L, Chiu C, Sun Y, Chen J, Khitrov G, Merckenschlager M, Holzman LB, Zhang W, Mundel P, Böttinger EP: Podocyte-selective deletion of *dicer* induces proteinuria and glomerulosclerosis. *J Am Soc Nephrol* 19: 2159–2169, 2008
31. Faul C, Donnelly M, Merscher-Gomez S, Chang YH, Franz S, Delfgaauw J, Chang JM, Choi HY, Campbell KN, Kim K, Reiser J, Mundel P: The actin cytoskeleton of kidney podocytes is a direct target of the anti-proteinuric effect of cyclosporine A. *Nat Med* 14: 931–938, 2008
32. Sethupathy P, Megraw M, Hatzigeorgiou AG: A guide through present computational approaches for the identification of mammalian microRNA targets. *Nat Methods* 3: 881–886, 2006
33. Grimson A, Farh KK, Johnston WK, Garrett-Engele P, Lim LP, Bartel DP: MicroRNA targeting specificity in mammals: determinants beyond seed pairing. *Mol Cell* 27: 91–105, 2007
34. Betel D, Wilson M, Gabow A, Marks DS, Sander C: The microRNA.org resource: targets and expression. *Nucleic Acids Res* 36: D149–D153, 2008
35. Wang X: miRDB: a microRNA target prediction and functional annotation database with a wiki interface. *RNA* 14: 1012–1017, 2008
36. Meng XM, Huang XR, Xiao J, Chen HY, Zhong X, Chung AC, Lan HY: Diverse roles of TGF- $\beta$  receptor II in renal fibrosis and inflammation in vivo and in vitro. *J Pathol* 227: 175–188, 2012
37. Sempere LF, Freemantle S, Pitha-Rowe I, Moss E, Dmitrovsky E, Ambros V: Expression profiling of mammalian microRNAs uncovers a subset of brain-expressed microRNAs with possible roles in murine and human neuronal differentiation. *Genome Biol* 5: R13, 2004
38. Chen JF, Mandel EM, Thomson JM, Wu Q, Callis TE, Hammond SM, Conlon FL, Wang DZ: The role of microRNA-1 and microRNA-133 in skeletal muscle proliferation and differentiation. *Nat Genet* 38: 228–233, 2006
39. Kutay H, Bai S, Datta J, Motiwala T, Pogribny I, Frankel W, Jacob ST, Ghoshal K: Downregulation of miR-122 in the rodent and human hepatocellular carcinomas. *J Cell Biochem* 99: 671–678, 2006
40. Esau C, Davis S, Murray SF, Yu XX, Pandey SK, Pear M, Watts L, Booten SL, Graham M, McKay R, Subramaniam A, Propp S, Lollo BA, Freier S, Bennett CF, Bhanot S, Monia BP: miR-122 regulation of lipid metabolism revealed by in vivo antisense targeting. *Cell Metab* 3: 87–98, 2006
41. Wienholds E, Kloosterman WP, Miska E, Alvarez-Saavedra E, Berezikov E, de Bruijn E, Horvitz HR, Kauppinen S, Plasterk RH: MicroRNA expression in zebrafish embryonic development. *Science* 309: 310–311, 2005
42. Beuvink I, Kolb FA, Budach W, Garnier A, Lange J, Natt F, Dengler U, Hall J, Filipowicz W, Weiler J: A novel microarray approach reveals new tissue-specific signatures of known and predicted mammalian microRNAs. *Nucleic Acids Res* 35: e52, 2007
43. Li R, Chung AC, Dong Y, Yang W, Zhong X, Lan HY: The microRNA miR-433 promotes renal fibrosis by amplifying the TGF- $\beta$ /Smad3-Azin1 pathway. *Kidney Int* 84: 1129–1144, 2013
44. Zhou H, Hasni SA, Perez P, Tandon M, Jang SI, Zheng C, Kopp JB, Austin H 3rd, Balow JE, Alevizos I, Illei GG: miR-150 promotes renal fibrosis in lupus nephritis by downregulating SOCS1. *J Am Soc Nephrol* 24: 1073–1087, 2013
45. Isono M, Chen S, Hong SW, Iglesias-de la Cruz MC, Ziyadeh FN: Smad pathway is activated in the diabetic mouse kidney and Smad3 mediates TGF- $\beta$ -induced fibronectin in mesangial cells. *Biochem Biophys Res Commun* 296: 1356–1365, 2002
46. Fujimoto M, Maezawa Y, Yokote K, Joh K, Kobayashi K, Kawamura H, Nishimura M, Roberts AB, Saito Y, Mori S: Mice lacking Smad3 are protected against streptozotocin-induced diabetic glomerulopathy. *Biochem Biophys Res Commun* 305: 1002–1007, 2003
47. Forrester E, Chytil A, Bieri B, Aakre M, Gorska AE, Sharif-Afshar AR, Muller WJ, Moses HL: Effect of conditional knockout of the type II TGF- $\beta$  receptor gene in mammary epithelia on mammary gland development and polyomavirus middle T antigen induced tumor formation and metastasis. *Cancer Res* 65: 2296–2302, 2005
48. Rojas A, Padidam M, Cress D, Grady WM: TGF- $\beta$  receptor levels regulate the specificity of signaling pathway activation and biological effects of TGF- $\beta$ . *Biochim Biophys Acta* 1793: 1165–1173, 2009
49. Gewin L, Bulus N, Mernaugh G, Moeckel G, Harris RC, Moses HL, Pozzi A, Zent R: TGF- $\beta$  receptor deletion in the renal collecting system exacerbates fibrosis. *J Am Soc Nephrol* 21: 1334–1343, 2010
50. Shen N, Lin H, Wu T, Wang D, Wang W, Xie H, Zhang J, Feng Z: Inhibition of TGF- $\beta$ 1-receptor posttranslational core fucosylation attenuates rat renal interstitial fibrosis. *Kidney Int* 84: 64–77, 2013
51. Schnaper HW, Hayashida T, Poncelet AC: It's a Smad world: regulation of TGF- $\beta$  signaling in the kidney. *J Am Soc Nephrol* 13: 1126–1128, 2002
52. Böttinger EP: TGF- $\beta$  in renal injury and disease. *Semin Nephrol* 27: 309–320, 2007
53. Lan HY: Diverse roles of TGF- $\beta$ /Smads in renal fibrosis and inflammation. *Int J Biol Sci* 7: 1056–1067, 2011
54. Chen X, Ba Y, Ma L, Cai X, Yin Y, Wang K, Guo J, Zhang Y, Chen J, Guo X, Li Q, Li X, Wang W, Zhang Y, Wang J, Jiang X, Xiang Y, Xu C, Zheng P, Zhang J, Li R, Zhang H, Shang X, Gong T, Ning G, Wang J, Zen K, Zhang J, Zhang CY: Characterization of microRNAs in serum: a novel class

- of biomarkers for diagnosis of cancer and other diseases. *Cell Res* 18: 997–1006, 2008
55. Guo G, Morrissey J, McCracken R, Tolley T, Klahr S: Role of TNFR1 and TNFR2 receptors in tubulointerstitial fibrosis of obstructive nephropathy. *Am J Physiol* 277: F766–F772, 1999
56. Bautista-García P, Reyes JL, Martín D, Namorado MC, Chavez-Munguía B, Soria-Castro E, Huber O, González-Mariscal L: Zona occludens-2 protects against podocyte dysfunction induced by ADR in mice. *Am J Physiol Renal Physiol* 304: F77–F87, 2013
57. Lan HY, Hutchinson P, Tesch GH, Mu W, Atkins RC: A novel method of microwave treatment for detection of cytoplasmic and nuclear antigens by flow cytometry. *J Immunol Methods* 190: 1–10, 1996

---

This article contains supplemental material online at <http://jasn.asnjournals.org/lookup/suppl/doi:10.1681/ASN.2015040422/-/DCSupplemental>.